

UCP2 Modulates Cell Proliferation through the MAPK/ERK Pathway during Erythropoiesis and Has No Effect on Heme Biosynthesis^{*[5]}

Received for publication, July 16, 2008 Published, JBC Papers in Press, August 7, 2008, DOI 10.1074/jbc.M805400200

Alvaro Elorza^{‡§1}, Brigham Hyde^{‡§}, Hanna K. Mikkola[¶], Sheila Collins^{||2}, and Orian S. Shirihai^{‡§1,3}

From the [‡]Department of Pharmacology and Experimental Therapeutics, Tufts University School of Medicine, Boston, Massachusetts 02111, [¶]Department of Molecular, Cell and Developmental Biology, University of California Los Angeles, Los Angeles, California 90095, and ^{||}The Hamner Institutes for Health Sciences, Research Triangle Park, North Carolina 27709, and [§]Evans Biomedical Research Center, Boston University, Boston, Massachusetts 02118

UCP2, an inner membrane mitochondrial protein, has been implicated in bioenergetics and reactive oxygen species (ROS) modulation. High levels of UCP2 mRNA were recently found in erythroid cells where UCP2 is hypothesized to function as a facilitator of heme synthesis and iron metabolism by reducing ROS production. We examined UCP2 protein expression and role in mice erythropoiesis *in vivo*. UCP2 was mainly expressed at early stages of erythroid maturation when cells are not fully committed in heme synthesis. Iron incorporation into heme was unaltered in reticulocytes from UCP2-deficient mice. Although heme synthesis was not influenced by UCP2 deficiency, mice lacking UCP2 had a delayed recovery from chemically induced hemolytic anemia. Analysis of progenitor cells from bone marrow and fetal liver both *in vitro* and *in vivo* revealed that UCP2 deficiency results in a significant decrease in cell proliferation at the erythropoietin-dependent phase of erythropoiesis. This was accompanied by reduction in the phosphorylated form of ERK, a ROS-dependent cytosolic regulator of cell proliferation. Analysis of ROS in UCP2 null erythroid cells revealed altered distribution of ROS, resulting in decreased cytosolic and increased mitochondrial ROS. Restoration of the cytosol oxidative state of erythroid progenitor cells by the pro-oxidant Paraquat reversed the effect of UCP2 deficiency on cell proliferation in *in vitro* differentiation assays. Together, these results indicate that UCP2 is a regulator of erythropoiesis and suggests that inhibition of UCP2 function may contribute to the development of anemia.

Uncoupling proteins (UCPs)⁴ are members of the anion carrier protein family located in the inner membrane of mitochondria.

* This work was supported, in whole or in part, by National Institutes of Health Grants 1-R01-DK-074778-01 and 5-R01-HL-071629-03. The costs of publication of this article were defrayed in part by the payment of page charges. This article must therefore be hereby marked "advertisement" in accordance with 18 U.S.C. Section 1734 solely to indicate this fact.

[5] The on-line version of this article (available at <http://www.jbc.org>) contains supplemental Figs. S1–S5 and Table 1.

¹ Supported by National Institutes of Health Grant 5-R01-HL-071629-03.

² Supported by National Institutes of Health Grant R01-DK-54024.

³ To whom correspondence should be addressed: Boston University, Evans Biomedical Research Center, 650 Albany St., Boston, MA 02118. Tel.: 617-230-8570; E-mail: Shirihai@bu.edu.

⁴ The abbreviations used are: UCP, uncoupling proteins; EPO, erythropoietin; ROS, reactive oxygen species; ERK, extracellular signal-regulated kinase; P-ERK, phosphorylated ERK; MAPK, mitogen-activated protein kinase; WT, wild type; RBC, red blood cells; PBS, phosphate-buffered saline; PH, phenylhydrazine; FACS, fluorescence-activated cell sorting; KO, knock-out; BFU-E, erythroid burst-forming units; CFU-E, erythroid colony-forming units; TBAP, Mn(III) tetrakis (4-benzoic acid) porphyrin chloride.

At least in the case of UCP1, it has been demonstrated that the protein disseminates the proton gradient across the mitochondrial inner membrane and generates heat (1–5).

UCP2 was first described by Fleury *et al.* (6). It shares 59% identity to UCP1 and is expressed most abundantly in mitochondria from spleen, certain regions of the brain, the pancreas, macrophages (6–8), and mast cells.⁵ In contrast to UCP1, its function has not been related to heat production but, rather, to the control of reactive oxygen species (ROS) production (9–13). UCP2 is induced by treatments that elevate ROS, and its induction can be inhibited by antioxidants (8, 14). Expression of UCP2 has been shown to result in a decrease in mitochondrial superoxide (9, 10, 15–18). UCP2 has been shown to have a protective effect in brain, preventing acute damage produced by ischemia (19–22), in the circulatory system, preventing atherosclerotic plaques (23), and in cardiomyocytes, where its overexpression is anti-apoptotic (12). Other studies have shown that UCP2 acts in macrophages and pancreatic beta cells as a regulator of secretion, affecting the killing capacity and glucose-induced insulin secretion, respectively (9, 16, 24–26).

We have previously shown that UCP2 is induced as a result of GATA-1 activation in the proerythroblast cell line, G1E-ER (27). UCP2 may play a protective role during erythroid differentiation where ROS may be generated by the large quantities of iron imported into the mitochondria during the process of heme biosynthesis (28). Indeed, mitochondrial oxidative stress was found to play a key role in sideroblastic anemia and the myelodysplastic syndrome in humans and in zebrafish (29–31). The importance of controlling ROS generation during erythropoiesis is also demonstrated by the severe hematopoietic phenotype of SOD2 null embryos and by the hemolytic anemia of the peroxiredoxin II null mice (32–37). Additionally, it has been proposed that through uncoupling, UCP2 may facilitate heme synthesis by creating a local low oxygen environment in the mitochondrial matrix (29), thereby maintaining iron in the reduced ferrous iron (Fe²⁺) state, keeping it available for ferrochelatase. Although it has been proposed that UCP2 plays a role in heme synthesis during erythroid differentiation, this hypothesis has not been tested thus far.

wild type; RBC, red blood cells; PBS, phosphate-buffered saline; PH, phenylhydrazine; FACS, fluorescence-activated cell sorting; KO, knock-out; BFU-E, erythroid burst-forming units; CFU-E, erythroid colony-forming units; TBAP, Mn(III) tetrakis (4-benzoic acid) porphyrin chloride.

⁵ M. Tagen, A. Elorza, W. Boucher, C. Kopley, O. S. Shirihai, and T. C. Theoharides, unpublished results.

UCP2 Function in Erythropoiesis

In the present study we have examined the role of UCP2 during the process of erythropoiesis using UCP2 null mice. Although we found that deficiency of UCP2 does not affect heme biosynthesis, UCP2 null mice exhibited a lower proliferation rate of the proerythroblasts and early basophilic erythroblasts during the EPO-dependent phase. Interestingly, our results indicate that UCP2 is modulating proliferation through ERK, a signaling pathway that has been implicated in cell proliferation during erythropoiesis and is regulated by ROS (38–40).

EXPERIMENTAL PROCEDURES

Cell Lines—G1E-ER cells were cultured in Iscove's modified Dulbecco's media (Invitrogen-Invitrogen) containing 15% heat inactivated fetal bovine serum, 2% pen/strep (Invitrogen), 120 nM monothioglycerol (Sigma), 2 units/ml EPO (StemCell Tech), and 50 ng/ml SCF/KL (StemCell Tech). Cell density was kept below 1×10^6 cells/ml. Upon activation of GATA-1 by 10^{-6} M β -estradiol, G1E-ER cells undergo synchronous cell cycle arrest followed by terminal erythroid maturation.

Animals—12–16-week-old UCP2 KO (9) and wild type (WT, The Jackson Laboratory) C57BL/6J mice were used. All procedures were performed in accordance with the Institutional Guidelines for Animal Care at Tufts University (IACUC no. 11-04) in compliance with United States Public Health Service Regulations.

Bone Marrow and Fetal Liver Isolation—Fetal liver cells were isolated from E13.5 UCP2 KO and WT embryos and mechanically dissociated by pipetting in isolation media (Iscove modified Dulbecco's medium, 2% fetal bovine serum). Bone marrow cells were harvested by flushing femurs with isolation media. Single-cell suspensions were prepared by drawing medium and cells up and down through a 1-ml syringe and 27-gauge needle and then passed through 40- μ m cell strainers (41, 42).

Osmotic Fragility Assay—Osmotic fragility of erythrocytes was measured on freshly collected blood from 12–16-week-old UCP2 KO and WT mice. Red blood cells (RBCs) were washed with PBS and suspended in varying concentrations of NaCl. Samples were incubated at room temperature for 30 min and centrifuged at $1500 \times g$ for 10 min at 4 °C. The supernatant was collected, and absorbance was measured at 540 nm with appropriate controls. The lysis percentage of RBCs was calculated from the absorbance, and a fragility curve was generated by plotting varying salt concentrations versus hemolysis (43, 44).

Induction of Hemolytic Anemia with Phenylhydrazine—Mice received intraperitoneal injections of 50 mg phenylhydrazine (PH)/kg body weight on experimental days 0, 1, and 3. PH chloride (Sigma) was dissolved in PBS (5 μ g/ μ l) and filtered through 0.22- μ m membrane. Blood and bone marrow were collected for analysis on experimental days 0, 3, 6, and 9 unless stated otherwise (41, 45).

^{59}Fe Heme Incorporation—Heme incorporation was performed as described in Zhang *et al.* (46). Briefly, mice reticulocytes were exposed to 2 μ M [^{59}Fe]transferrin on ice to saturate membrane receptors. Endocytosis was allowed by transferring the samples to 37 °C. Total protein fraction was obtained and precipitated in 10% trichloroacetic acid for 15 min at 4 °C and washed twice in 7% trichloroacetic acid. ^{59}Fe radioactivity

counting was performed in both pellet and supernatant fractions utilizing the 1470 WIZARD automatic gamma counter (PerkinElmer Life Sciences). Percentage of iron incorporated into heme fraction was calculated as follows: (^{59}Fe pellet/reticulocyte number) \times 100/((^{59}Fe pellet + ^{59}Fe supernatant)/reticulocyte number). $^{59}\text{FeCl}_3$ was purchased from Amersham Biosciences (Buckinghamshire, UK), Apo-Tf (Sigma) was labeled with ^{59}Fe using ^{59}Fe -labeled citrate as described in Martinez-Medellin and Schulman (47).

Fluorescence-activated Cell Sorting (FACS) Analysis—Bone marrow or fetal liver cells ($\sim 1 \times 10^5$) were immunostained simultaneously with phycoerythrin-conjugated anti-TER119 (1:100) (BD Pharmingen) and fluorescein isothiocyanate-conjugated anti-CD71 (1:100) (BD Pharmingen) and either allophycocyanin-conjugated anti-C-KIT (1:100) (BD Pharmingen) antibodies in FACS buffer (PBS, 1% bovine serum albumin) as previously described (41) or annexin V (3:100) (APC-conjugated, BD Pharmingen). For apoptosis analysis the polycaspases FLICA (6-carboxyfluorescein-VAD-fluoromethyl ketone) substrate (Immunochemistry Technologies, LLC) was used according to manufacturer's instructions. Flow cytometry was performed using a FACSCalibur (BD Bioscience), and R1-R5 gating was selected according to Rooke and Orkin (48). FACS data analysis was performed with FACS Express V3 software. Cell debris was excluded by gating on the forward and side scatter plot.

Erythroid Differentiation in Vitro—Total fetal liver or bone marrow cells previously treated with ACK lysis buffer (0.8% NH_4Cl , 0.1 mM EDTA, Stemcell Technologies, Vancouver, BC, Canada) were labeled with biotin-conjugated anti-TER119 or anti C-KIT antibody (1:100) (BD Pharmingen), respectively. TER119 $^-$ or C-KIT $^+$ cells were purified through a StemSep column as per the manufacturer's instructions (StemCell Technologies). Purified cells were seeded in fibronectin-coated wells (BD Discovery Labware) at a cell density of 1×10^5 /ml. On the first day the purified cells were cultured in Iscove's modified Dulbecco's medium supplemented with 15% fetal bovine serum, 20% BIT 9500 (StemCell Technologies), 10^{-4} M β -mercaptoethanol, and 2 units/ml EPO (Amgen, Thousand Oaks, CA). On the second day this medium was replaced with erythroid differentiation media according to Zhang *et al.* (41).

Mitochondrial Isolation—Mitochondrial isolation was achieved using a mitochondrial isolation kit for tissue (Pierce, catalog #89801) following the manufacturer's instructions.

Protein Oxidation Detection—To detect oxidized proteins we used the OxyblotTM protein oxidation detection kit (Chemicon International) according to manufacturer's manual. It is based on detection of carbonyl groups which are introduced into protein side chains when proteins are exposed to oxidative stress.

Reactive Radical Species Detection—Bone marrow was collected as described, and 1×10^6 cells were stained with 5 μ M dihydroethidium (Invitrogen) or MitoSox (Invitrogen) for 30 min at 37 °C. MitoSox-stained samples were also treated simultaneously with 10 μ M Verapamil (Sigma-Aldrich). After the incubation time, cells were washed twice in warm FACS buffer and immunostained with fluorescein isothiocyanate-conjugated anti-CD71 antibody as described above and analyzed by FACS.

Western Blot—Samples were prepared according to Kefaloyianni *et al.* (49) and fractionated in 12% polyacrylamide gel and transferred onto a polyvinylidene difluoride membrane using a semidry transfer machine. UCP2 (Santa Cruz), Porin (Calbiochem), β -actin (Novus Biologicals), Complex III (Mitosciences), and ERK (Cell signaling) antibodies were used according to manufacturer's instruction.

Statistical Analysis—Data were analyzed by Student's *t* test or analysis of variance ($\alpha = 0.05$) with the GraphPad Prism software.

RESULTS

UCP2 Expression in Erythroid Cells—If UCP2 is involved in heme synthesis, we expected the expression levels of the protein to peak when cells are heavily involved in heme production. UCP2 expression was analyzed in three main populations of primary erythropoietic cells; Ter119 negative (BFU-E, CFU-E, proerythroblast; not actively involved in heme synthesis), Ter119 positive cells (early and late basophilic erythroblasts; involved in heme synthesis; highly proliferative), and reticulocytes (actively involved in heme synthesis; non proliferative). Ter119⁺ and Ter119⁻ cells were derived from E13.5 fetal livers and reticulocytes from the peripheral blood of PH-treated mice as described ("Experimental Procedures"). Unexpectedly, UCP2 protein was expressed in the early progenitors (Ter119⁻) and reached its maximum level of expression in the basophilic erythroblasts (Ter119⁺). Reticulocytes expressed very low levels of UCP2 (Fig. 1A).

To determine the temporal relationship between UCP2 expression and heme production, we investigated the kinetics of UCP2 protein expression in G1E-ER cells. G1E-ER cells are arrested at proerythroblast stage due to the lack of endogenous GATA-1 and, thus, offer an excellent model to track early erythroid differentiation. After induction with β -estradiol, cells were collected at 0, 12, 24, 48, and 72 h, and UCP2 expression was analyzed. Interestingly, UCP2 protein peaks at 12 h and decreases thereafter ($p = 0.0084$ for the decrease between 12 and 48 h, Fig. 1B). The induction of UCP2 during the first 12–24 h correlates with early erythropoiesis, which is characterized by an increased rate of cell division and very limited hemoglobin synthesis (50). At 48 h cells no longer divide and are at the stage characterized by high hemoglobin synthesis activity. The biphasic pattern of UCP2 expression in G1E-ER cells reflects the pattern found in primary cells during the transition from Ter119⁻ to reticulocytes. This pattern of induction early in erythroid differentiation also supports that UCP2 expression is induced by the GATA-1 transcription factor.

UCP2 Function in Erythropoiesis—To determine the role of UCP2 in erythropoiesis *in vivo*, WT and UCP2 KO C57BL/6J mice were induced to develop hemolytic anemia, and the progression of reticulocytosis was monitored. Thirty male mice (12–16-week-old) were injected intraperitoneally with 50 mg/kg PH and 10 mice with PBS (control) at experimental days 0 (D0), 1 (D1), and 3 (D3), and samples were collected at D0, D3, D6, and D9 ($n = 5$ per treatment). Blood profile was analyzed at 3 different stages: (i) immediately before treatment (D0), (ii) acute marrow response (D3), and (iii) recovery phase (D6 and D9).

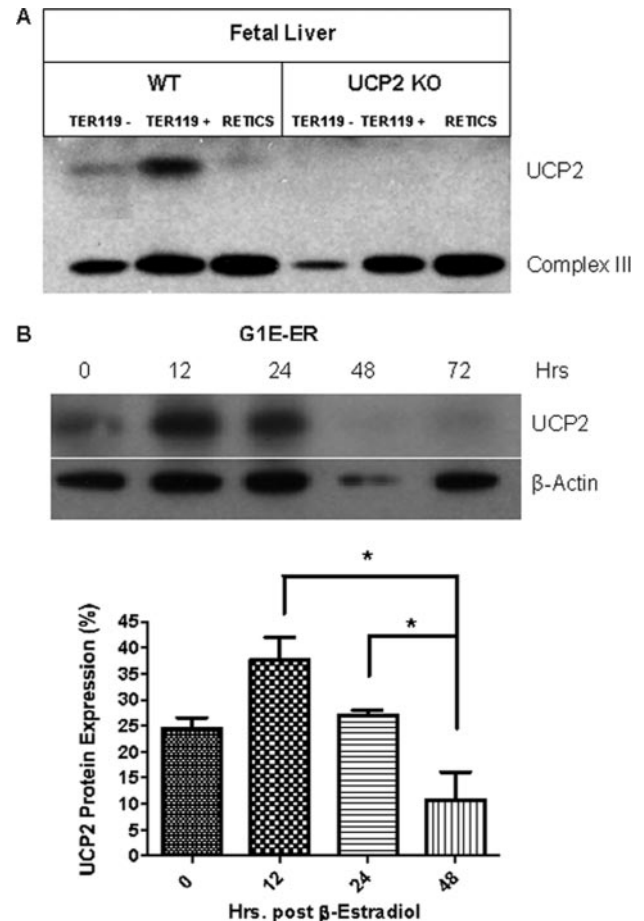


FIGURE 1. Expression of UCP2 in erythropoietic cells. A, E13.5 Fetal livers from WT and KO mice were treated with ACK lysis buffer to eliminate hemoglobin containing cells (mainly chromatophilic erythroblasts and reticulocytes). Ter119⁻ (BFU-E, CFU-E and proerythroblasts) and Ter119⁺ (early and late basophilic erythroblast) cells were then isolated using anti-Ter119 antibody. Reticulocytes were obtained from peripheral blood at day 6 post-induction of hemolytic anemia with phenylhydrazine. Reticulocyte content was 50–70%. Samples were analyzed by Western blot. Maximal expression of UCP2 was seen in the Ter119⁺ samples and was minimal in reticulocytes (RETICS). Complex III of the mitochondrial respiratory chain was used as loading control. B, kinetic study of UCP2 expression during differentiation of the inducible proerythroblast cell line, G1E-ER. After induction of differentiation with 1×10^{-6} M β -estradiol, samples were collected at 0, 12, 24, 48, and 72 h and analyzed by Western blot (upper panel). UCP2 is induced during the first 12 h of differentiation and decreases thereafter. This expression pattern correlates with the proliferation phase (0–24 h) and the onset of hemoglobin synthesis, respectively. β -Actin was used as loading control. Lower panel, densitometry analysis of UCP2 expression during G1E-ER differentiation. ($p = 0.0084$, one way analysis of variance).

At D0 (PBS-injected mice) WT and UCP2 KO mice presented a similar complete blood count profile, and the PH treatment resulted in an acute decline in RBC count, hematocrit, and hemoglobin in both genotypes (supplemental Fig. S1). The acute marrow response was characterized by reticulocytosis that developed on D3 (Fig. 2A). During this phase, reticulocyte production was attenuated in the UCP2 KO and reached only 47.22% that of the WT ($p = 0.0271$). During the recovery phase, reticulocyte count of UCP2 and WT reached similar values. This difference in kinetics supports a UCP2 role in expansion rather than maturation of the erythroid cells. Serum chemistry analysis was also performed, and no differences were found between UCP2 KO and WT mice (supplemental Table S1).

UCP2 Function in Erythropoiesis

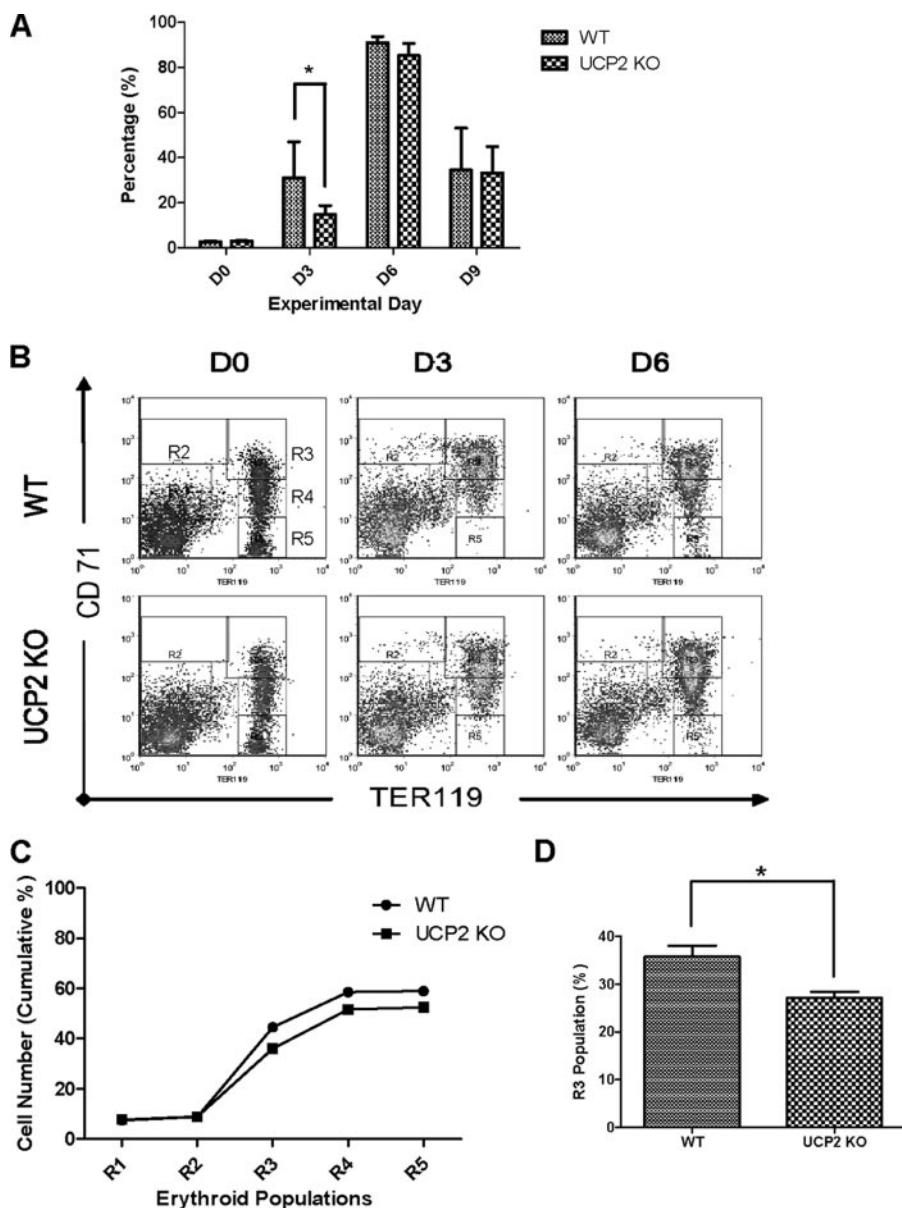


FIGURE 2. Erythropoietic response of UCP2 KO and WT mice to PH-induced hemolytic anemia. Mice were injected with 50 mg/K PH at D0, D1, and D3 and samples collected at D0, D3, D6, and D9. *A*, peripheral blood analysis of reticulocyte percentage. Both genotypes increased reticulocyte percentage throughout the course of the experiment. However, UCP2 KO mice exhibited a reduced level during the acute marrow response phase (D3) ($p = 0.0271$, one-tailed Mann-Whitney test, $n = 40$; 5 mice per experimental day and per genotype). Error bars represent S.D. See also Fig. S2. *B*, bone marrow analysis. Five erythroid populations from immature to mature (R1, R2, R3, R4, and R5) are distinguished by CD71 and TER119 expression levels in freshly isolated marrow by flow cytometry. Note that control samples D0 are characterized by a minor R2 and a large R5 population. During PH-induced acute marrow response D3, R5 disappears and R2 increases. At the recovery phase D6, R5 is restored. *C* and *D*, quantitative analysis of cell progression in acute marrow response D3. *C*, cumulative percentage at each erythroid population, i.e. R1 = R1; R2 = R1 + R2; R3 = R1 + R2 + R3 and so on. The curve represents both expansion and maturation throughout erythropoiesis. UCP2 KO mice are characterized by reduced expansion at the R2-R3 stage. *D*, statistical analysis of R3 population, not cumulative ($p = 0.0040$, two-tailed Student's *t* test).

To determine the mechanism responsible for the attenuated acute marrow response, we analyzed the response of bone marrow progenitors to PH treatment in terms of differentiation, expansion, maturation, and survival.

Differentiation and maturation of erythroid progenitors was determined by FACS analysis of the relative size of five populations of cells that were identified by the expression of a combi-

nation of the membrane markers CD71 and TER119 (Fig. 2*B*). The five cell populations represent primitive progenitor cells, including BFU-E and CFU-E (R1, CD71^{med}, TER119^{low}), proerythroblasts and early basophilic erythroblasts (R2, CD71^{high}, TER119^{low}), early and late basophilic erythroblasts (R3, CD71^{high}, TER119^{high}), polychromatophilic erythroblasts (R4, CD71^{med}, TER119^{high}) and orthochromatophilic erythroblasts (R5, CD71^{low}, TER119^{high}) (41, 45, 48) as shown in Fig. 2*B*. Note that in the PH-induced acute marrow response (D3), the R5 population is decreased, and R2 population is increased. R5 reappears at the recovery phase (D6), and by D9 it is fully recovered (supplemental Fig. S2). Bone marrow cell expansion and maturation throughout erythropoiesis are presented as cumulative percentage of each erythroid population (Fig. 2*C*). The acute marrow response at D3 is delayed at the level of R2-R3 populations in the UCP2 KO mice (Fig. 2*C*). Further analysis showed that R3 was reduced by 24.19% ($p = 0.0040$) in the KO mice as compared with WT (Fig. 2*D*). This reduction in R3 was not due to increased cell death or reduced number of earlier progenitors BFU-E and CFU-E. FACS analysis of C-KIT⁺ cells (supplemental Fig. S2) and colony assay in methylcellulose (data not shown) did not show a reduction in the amount of BFU-E or CFU-E. Analysis of annexin V staining did not demonstrate any increase in the rate of apoptosis (supplemental Fig. S2).

The possibility that UCP2 deficiency inhibits the generation of R3 was tested using a two step *in vitro* differentiation assay. C-KIT⁺ cells were isolated from UCP2 KO and WT bone marrow samples and allowed to differentiate over 2 days.

Cells were cultured in the presence of EPO to induce differentiation to late basophilic erythroblast, i.e. the R3 population. After the first 24 h, EPO was removed from the media, and R3 cells progressed until terminal maturation. *In vitro* differentiation revealed that C-KIT⁺ cells from UCP2 KO exhibit delayed maturation at stage R2-R3 (Fig. 3, *A* and *C*). The total number of erythroid cells after EPO induction was 14.36% less in UCP2

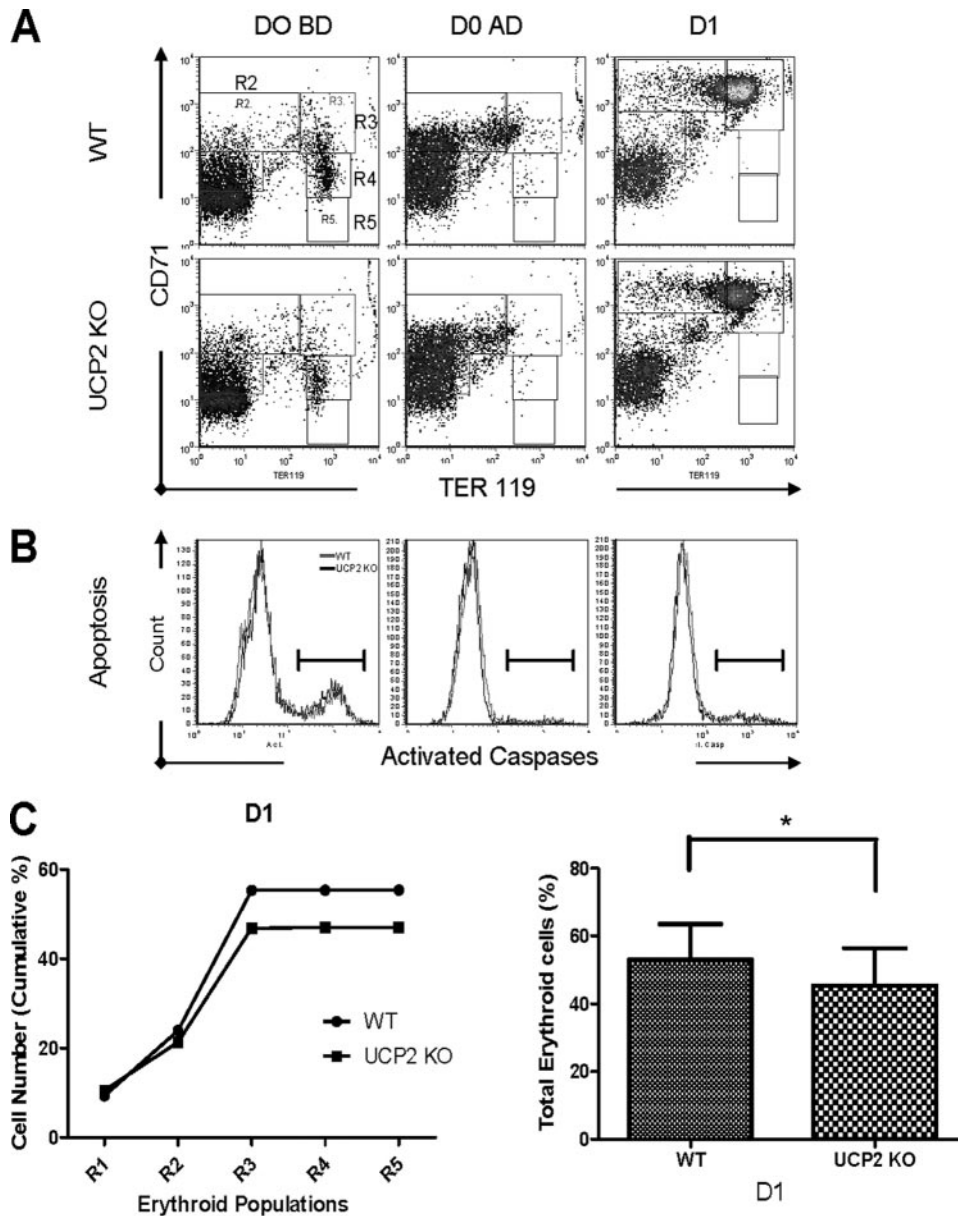


FIGURE 3. Kinetics of *in vitro* erythroid differentiation. C-KIT⁺ cells were isolated from bone marrow and were analyzed in a two stage *in vitro* differentiation assay. The first stage (0–24 h) was in the presence of EPO; the second stage (24–48 h) was in the absence of EPO (see “Experimental Procedures”). *A*, FACS dot plots as described in Fig. 2*B*. Cells were immunostained with fluorescein isothiocyanate-CD71 and phycoerythrin-TER119 to follow erythroid differentiation. *DO BD*, day 0 of fresh whole marrow; *DO AD*, day 0 of isolated C-KIT⁺ cells; *D1*, C-KIT⁺ cells cultured with EPO for 24 h. Note the propagation of cells from R2 to R3. *B*, analysis of apoptosis. Cells were stained with phycoerythrin-TER119 and FLICA (6-carboxyfluorescein-VAD-fluoromethyl ketone), a green fluorescent caspase substrate. No differences were found between the UCP2 KO and WT mice. *C*, quantitative analysis of cell progression. *Left panel*, cumulative percentage during the first 24 h (D1) at each erythroid population as described in Fig. 2*C* ($n = 4$). Note the same pattern of erythroid differentiation as compared with the marrow response (Fig. 2*C*). *Right panel*, statistical analysis of total erythroid cells (R1+R2+R3+R4+R5) at D1 ($p = 0.0307$, Student’s *t* test).

KO mouse as compared with WT ($p = 0.0307$, Fig. 3*C*, right panel). At day 2, EPO-independent maturation from R3 to R5 occurred at a similar rate in the two genotypes (supplemental Fig. S3). To determine whether cell loss through apoptosis contributes to the reduced total cell number in UCP2 KO, samples were stained with a fluorescent caspase-3 substrate to detect activated caspase-3 along with TER119 surface marker and analyzed by FACS. Fig. 3*B* shows that the rate of apoptosis was similar in the two genotypes, suggesting that apoptosis does not

contribute to the reduced cell number observed in UCP2 KO samples. The *in vitro* results (Fig. 3) match those obtained in the *in vivo* experiments (Fig. 2) and suggest that UCP2 affects cell proliferation during the EPO-dependent phase (R2–R3) of erythropoiesis.

Effect of UCP2 on Heme Biosynthesis, Globin Expression, and RBC Survival—Heme synthesis has been shown to be attenuated by increased oxidative environment (51). Because UCP2 might function to reduce ROS generation, we rationalized that its deficiency may affect heme and globin biosynthesis as well the stability of mature cells (43). To determine the effect of UCP2 deficiency on heme biosynthesis, we measured the rate of iron incorporation into heme in reticulocytes isolated from UCP2 KO and WT mice 7 days after induction of anemia. Reticulocyte samples were incubated for 0, 5, 10, and 30 min in the presence of [⁵⁹Fe]transferrin, and total iron incorporation into heme was determined. UCP2 KO reticulocytes did not show a reduced rate of iron incorporation into heme, indicating that UCP2 is neither essential nor rate-limiting in heme biosynthesis (Fig. 4*A*).

Expression of the different globin chains was determined using reverse transcription-PCR. Analysis of adult blood for α and β globins and E13.5 fetal liver for α , γ , and ζ globins revealed that the globin chain profile of the UCP2 KO mouse is unaltered (supplemental Fig. S4). Furthermore, UCP2 KO and WT mature red blood cells showed similar fragility, even though the higher oxidative stress in UCP2 KO is expected to result in increased resistance to the osmotic challenge (Fig. 4*B*).

The lack of effect of UCP2 deficiency on heme synthesis was in agreement with the lack of effect on mean corpuscular hemoglobin concentration (supplemental Fig. S1) and the absence of increased rate of apoptosis (supplemental Figs. S2 and S3).

Effect of UCP2 on Erythroid Cell ROS—UCP2 expression in cardiomyocytes and neurons has been shown to alter the levels of ROS (12, 13). We tested the levels of protein oxidation in isolated mitochondria and in whole cells from untreated bone marrow samples of UCP2 KO and WT (Fig. 5, *A* and *B*). Protein

UCP2 Function in Erythropoiesis

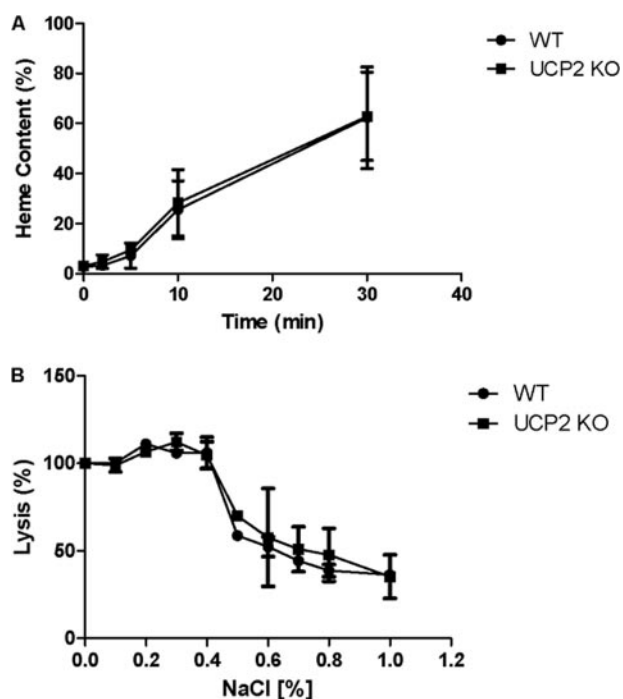


FIGURE 4. Effect of UCP2 on heme biosynthesis and RBC survival. A, ^{59}Fe incorporation into the heme fraction in reticulocytes. Data were normalized against reticulocyte number per sample and radioactivity in the non-protein fraction. No significant differences were found in iron incorporation rate between the two genotypes. B, osmotic fragility test. Peripheral blood was collected and exposed to different concentration of NaCl (%) for 30 min at room temperature. Hemolysis was assessed by spectrometry of supernatant at 540 nm. Cell oxidative damage is expected to increase the resistance to the insult, *i.e.* to shift the curve toward the left. No significant differences were found.

oxidation was determined by the occurrence of carbonyl groups in amino acid side chains as described under "Experimental Procedures." Bone marrow samples from UCP2 KO mice showed higher levels of protein oxidation in isolated mitochondria as compared with WT ($p = 0.0352$, Fig. 5A). Remarkably, however, total cellular protein oxidation from UCP2 KO was significantly reduced ($p = 0.0021$, Fig. 5B) as compared with WT. These findings suggested the possibility that mitochondrial ROS levels are increased, whereas cytosolic levels are decreased in UCP2 deficient cells. MitoSox and dihydroethidium were used to probe mitochondrial and cytosolic ROS, respectively, in CD71⁺ erythropoietic marrow cells (Fig. 5, C–E). In UCP2 KO cells, mitochondrial ROS was increased by 31.7% ($p = 0.0230$, one-tailed Student's *t* test), whereas cytosolic ROS was decreased by 14% ($p = 0.0314$, one-tailed Student's *t* test) as compared with WT cells. These results suggest that the intracellular distribution rather than the net production of ROS was altered by UCP2 deficiency in erythropoietic cells.

Effect of Oxidative Environment on Erythropoiesis—Our results suggested that altered distribution of ROS may influence red blood cell expansion. Thus, we tested whether chemically induced changes in redox environment can reverse the altered progression of erythropoiesis in the UCP2 deficient cells during the EPO-dependent phase. C-KIT⁺ bone marrow cells from UCP2 KO and WT mice were treated with the reductive agent, TBAP (a superoxide dismutase mimetic), or with the pro-oxidant, Paraquat, for 24 h in an *in vitro* differentiation

assay and analyzed by FACS (Fig. 6). Interestingly, 40 μM TBAP in both UCP2 KO and WT cells delayed cell maturation at the proerythroblast stage, which is seen as an increase in R2 but decrease in R3 (Fig. 6A). In addition, the total cell number of cells committed in erythropoiesis was also decreased (Fig. 6B). Conversely, 3 μM Paraquat caused the opposite effect, increasing the number of cells in the R2 population (Fig. 6A). The erythropoietic effect of Paraquat was particularly strong in the UCP2-deficient cells. Paraquat increased up to 14% ($p = 0.0494$) the total number of cells as compared with no treatment (Fig. 6B).

UCP2 and the MAPK Signaling Pathway—The control of cell proliferation during maturation from progenitors to late basophilic erythroblasts has been linked to the ERK signaling pathway (38). ERK is activated by phosphorylation during the EPO-dependent phase, and its activation is ROS-dependent (39, 52). We first determined ERK expression and phosphorylation in WT bone marrow TER119[−] and TER119⁺ cells marking the onset of the EPO-dependent and independent phases, respectively. Phosphorylated ERK (P-ERK), total ERK, and the mitochondrial protein Porin were detected by Western blot analysis (Fig. 7A). In agreement with published literature, P-ERK is abundant in TER119[−] cells. To determine ERK phosphorylation during the acute marrow response, ERK was analyzed in bone marrow samples from hemolytic anemia-induced UCP2 KO and WT mice at D0, D2, and D3. P-ERK was normalized to total ERK and Porin according to the expression $\text{P-ERK} \times \text{Porin}/\text{total ERK}^2$. Levels of phosphorylated ERK in UCP2 KO were significantly lower ($p = 0.0281$) than in WT at all experimental days analyzed (Fig. 7B). Total ERK on the other hand was increased in the UCP2 KO samples. Similar results were found in *in vitro* differentiation assays from E13.5 fetal liver TER119[−] cells. In E13.5 fetal livers, more than 90% of the TER119[−] cells are C-KIT⁺, *i.e.* erythroid progenitor cells (41). P-ERK was abundant in progenitors from both UCP2 KO and WT fetal livers. However, the levels of P-ERK were diminished in the UCP2 KO compared with WT when cells were induced to differentiate into TER119⁺ early and late stage basophilic erythroblasts for 24 h with EPO (Fig. 7C). The role of ERK during earlier stages of maturation was also demonstrated by the inhibition of ERK phosphorylation. C-KIT⁺ cells induced to differentiate *in vitro* in the presence of ERK inhibitor U0126 demonstrate that inhibition of ERK blocks cell proliferation but does not block maturation (supplemental Fig. S5A) and that UCP2 KO samples are more sensitive to ERK inhibition as compared with WT (supplemental Fig. S5B). The effect of UCP2 on ERK phosphorylation may explain the reduced proliferation rate of R2 and R3 populations and the lack of effect on terminal maturation.

DISCUSSION

Here we studied the function of UCP2 in erythropoiesis. We have previously reported that activation of the erythroid transcription factor GATA-1 in G1E-ER cells up-regulates expression of UCP2 mRNA (27). Recently, UCP2 transcription was reported in mouse fetal liver and in adult mouse reticulocytes, suggesting its involvement in erythropoiesis (53). Here we report increased UCP2 protein expression in primary proeryth-

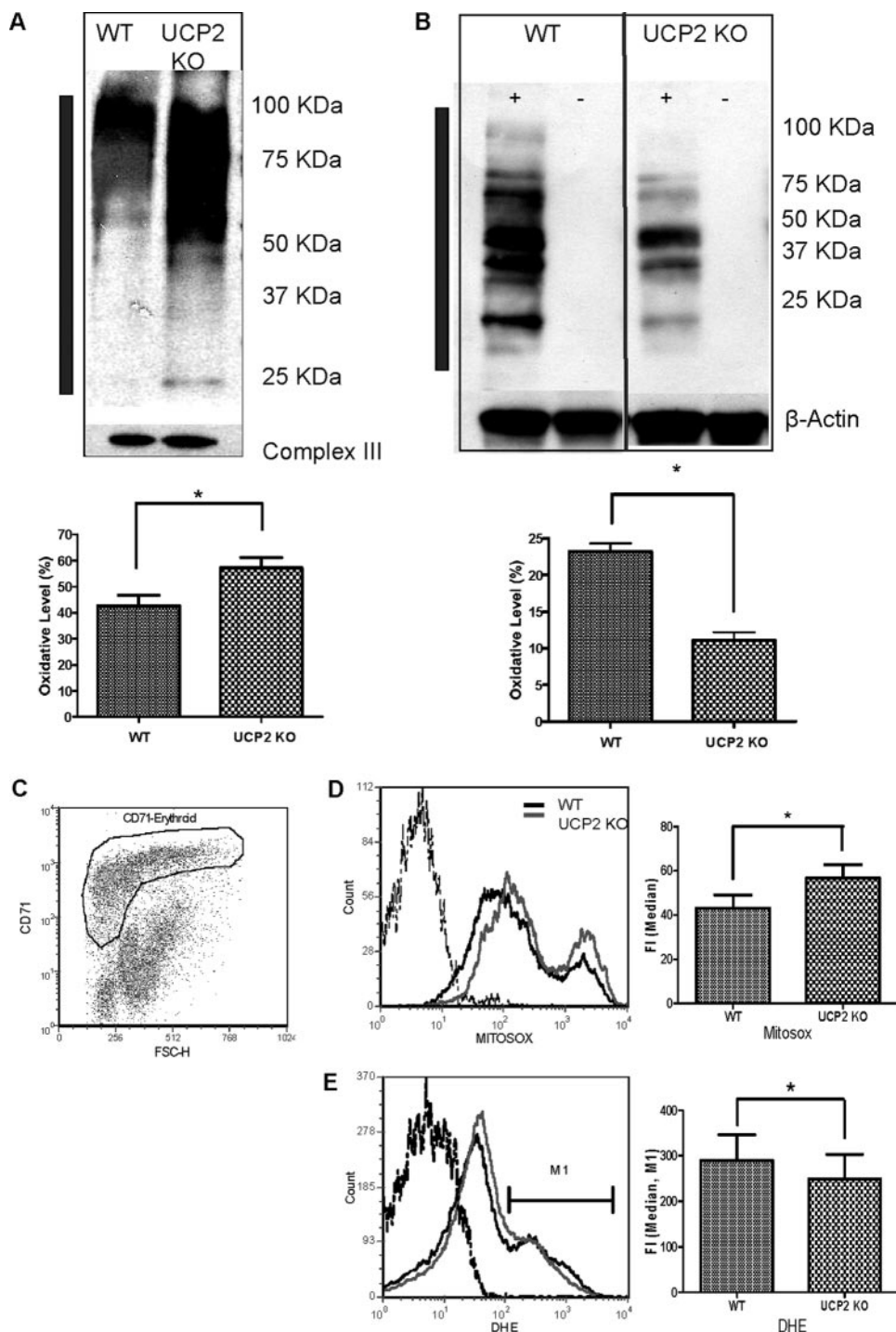


FIGURE 5. Effect of UCP2 on protein oxidation and ROS generation. *A* and *B*, analysis of oxidized protein in WT and UCP2 KO bone marrow samples. *A*, mitochondrial proteins. *B*, total cellular proteins. Samples were reacted with 2,4-dinitrophenylhydrazine to derivatize the protein carbonyl groups, which were then detected with an anti-2,4-dinitrophenol antibody after SDS-PAGE. +, positive derivatization; -, negative control of derivatization. Complex III and β -actin were used as loading control. Densitometry analysis was calculated by measuring all protein intensities along the left-side gray bar. Note that UCP2 KO is more oxidized at the mitochondria level ($p = 0.0352$, Student's *t* test) but surprisingly less at the total protein level ($p = 0.0021$, Student's *t* test) as compared with WT. *C*, *D*, and *E*, ROS generation by erythropoietic cells. Mitochondrial and cytosolic ROS were analyzed in bone marrow CD71⁺ erythroid cells selected by gating shown in *C* according to fluorescein isothiocyanate-CD71 antibody staining and Forward Scatter parameter (FSC-H) of bone marrow samples. *D*, superoxide levels inside mitochondria were determined by the mitochondrial superoxide probe, MitoSox ($p = 0.0230$, one-tailed Student's *t* test). *E*, cellular ROS levels were determined by dihydroethidium (DHE), which mainly identifies cytosolic superoxide radicals ($p = 0.0314$, one-tailed Student's *t* test). Dashed curves in *C* and *D* represent control unstained cells. Because of the low overall dihydroethidium fluorescence intensity, the M1 region was used for densitometry. Error bars represent S.D.

roblasts and basophilic erythroblasts from E13.5 fetal livers, differentiation stages that feature high cell division rates (45, 54). On the other hand, in cells that are heavily involved in heme synthesis, such as reticulocytes, UCP2 expression was hardly detectable. In contrast to protein levels, UCP2 mRNA is elevated in reticulocytes, indicating that expression patterns of UCP2 protein do not correlate with mRNA levels at different stages of blood cell development (53). Mis-correlation of UCP2 protein and mRNA was previously shown to be mediated by regulation of UCP2 translation (8). Kinetic studies in the erythropoietic cell line G1E-ER showed similar protein expression profile after induction of differentiation with β -estradiol. UCP2 protein increases 12 h after activation and declines thereafter, correlating with cell proliferation and the early stage of hemoglobinization. After 24 h post-induction, G1E-ER cell proliferation is arrested, and hemoglobin synthesis achieves maximal levels (50). Together, these findings indicate that UCP2 protein expression is higher at pre- and early hemoglobinization stages, when high levels of ROS are not expected, and is down-regulated at later stages when hemoglobinization occurs at its highest rate.

To examine the role of UCP2 in erythropoiesis, we chemically induced hemolytic anemia in UCP2 KO and WT mice and followed their recovery, monitoring the development of reticulocytosis during the acute marrow response. UCP2 KO mice had a slower recovery evidenced by slower development of reticulocytosis. Potential involvement of UCP2 at early and late stages of erythropoiesis was addressed. UCP2 deficiency did not affect late stages of maturation as demonstrated by normal rate of heme synthesis, hemoglobin content, and physical stability of the mature erythrocyte. The role of UCP2 during differentiation at early stages of maturation of RBC was assessed in bone marrow of PH-

UCP2 Function in Erythropoiesis

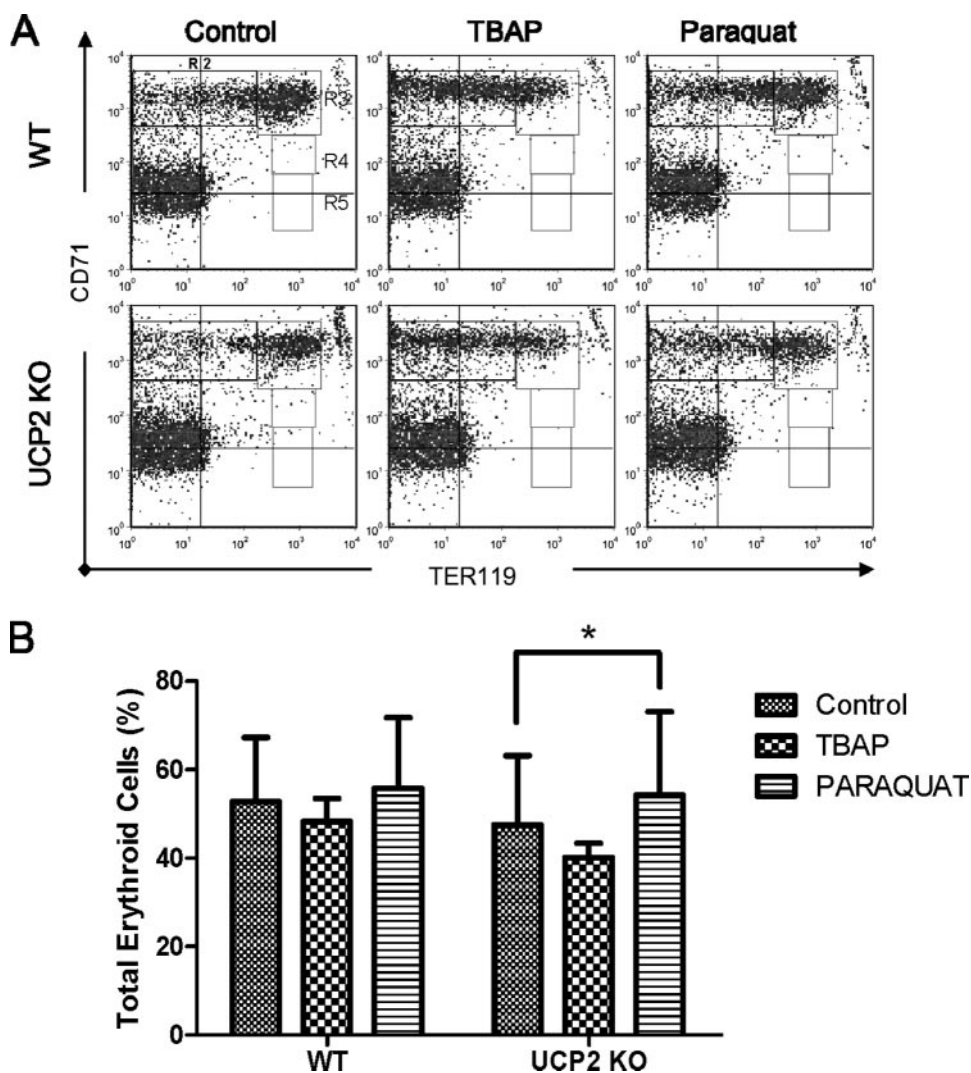


FIGURE 6. Effect of oxidative/reductive environment on the kinetics of *in vitro* erythroid differentiation. C-KIT⁺ cells isolated from bone marrow were cultured in the presence or absence of 40 μ M TBAP (anti-oxidant; SOD2 mimetic) or 3 μ M Paraquat (pro-oxidant) during the EPO-dependent phase (first 24 h). Samples were collected as described in Fig. 3 and immunostained with fluorescein isothiocyanate-CD71 and phycoerythrin-TER119 to follow erythroid differentiation by FACS. *A*, FACS dot plots at D1 as described in Fig. 2*B* under different culture conditions. Note that cell number in R2 and R3 is reduced in UCP2 KO as compared with WT under untreated (*Control*) conditions. TBAP inhibits progression from R2 to R3, indicated by the accumulation of cells in R2 in both genotypes. Treatment with paraquat resulted in the restoration of the reduced R2 and R3 populations of the UCP2 KO sample, whereas in WT it had comparatively little effect. *B*, quantification of the effect of TBAP and Paraquat on total erythroid cells. Paraquat treatment significantly increases the number of erythropoietic cells in UCP2 KO samples as compared with control ($p = 0.0494$, one-tailed T-Student). After treatment with paraquat, UCP2 KO cells show no significant differences as compared with untreated WT cells. (Control, $n = 7$; TBAP, $n = 3$; Paraquat $n = 4$). Error bars represent S.D.

treated mice. Analysis by FACS using CD71 and TER119 cell membrane markers to follow RBC maturation (41) displayed a lower percentage of R3 population (early and late basophilic erythroblasts) at D3 in UCP2 KO mice as compared with WT. Although increased apoptosis in R3 population could explain this result, annexin V staining ruled out this possibility. Assessment of the amount of early progenitors by FACS and colony assays showed that the number of BFU-E and CFU-E were similar in the two genotypes. Thus, UCP2 function and expression appears to be limited to the EPO-dependent phase, taking place from CFU-E to the late basophilic erythroblast stage (55, 56). The possibility that the effects of UCP2 deficiency were indirectly mediated by non erythroid cells responding to lack of

UCP2 was ruled out in *in vitro* differentiation experiments of marrow C-KIT⁺ cells, which displayed a similar delay in maturation during the first 24 h (EPO-dependent phase), again resulting in a decrease in R3 population. Our data demonstrate that UCP2 protein induction and UCP2 KO phenotype is strongest during early erythropoiesis during the EPO dependent phase and suggest that its function as a ROS modifier (9, 10, 16, 57) might influence erythroid proliferation.

Proliferation signaling pathways such as Rb/E2F, c-Myc, and Ras are characterized by their ability to activate nuclear transcription factors located in the cytosol (58). If UCP2 is involved in cell proliferation, it is imperative that the signal generated within mitochondria is exported to the cytosol to effect a nuclear response. Evidence of UCP2 function in signal transduction was first suggested by the activation of the IKK and the NF- κ B cascade in macrophages from UCP2 KO mice (16). This effect was inhibited when macrophages were treated with ROS inhibitors superoxide dismutase and catalase, indicating that lack of UCP2 results in greater O₂⁻/H₂O₂ release from mitochondria. Indeed, H₂O₂ serves as an activator of NF- κ B (59).

We have shown here that mitochondria of UCP2 KO bone marrow contain increased concentrations of superoxide radical which is accompanied by higher levels of oxidized proteins as compared with WT. This agrees with Bai *et al.* (16), who found spleen mitochondria from UCP2 KO to contain twice the

amount of H₂O₂ as compared with WT basal conditions. Interestingly, the cytosolic ROS and the total cellular levels of oxidized protein were reduced in UCP2 KO. One explanation for this finding is that erythroid UCP2 protein modulates the distribution of reactive radicals between mitochondria to cytosol. This is consistent with prior studies which demonstrated that overexpression (20) or knockdown (60) of UCP2 does not affect the net generation of ROS by mitochondria. Rather, expression of UCP2 shifted ROS from the mitochondrial matrix to the cytosolic side of the inner mitochondrial membrane (20).

To test whether this ROS relocation from mitochondria to cytosol can influence the expansion of erythropoietic cells, we challenged marrow C-Kit⁺ cells to undergo *in vitro* differenti-

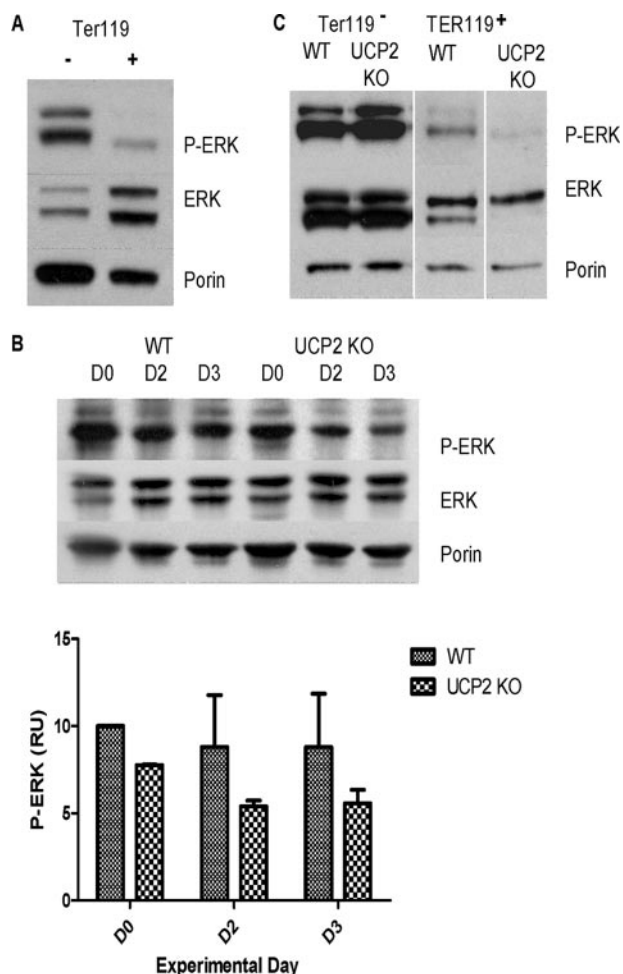


FIGURE 7. Effect of UCP2 on the levels of phosphorylated ERK in erythropoiesis. A, control levels of phosphorylated ERK 1/2 (or ERK 44/42) in WT bone marrow TER119⁻ and TER119⁺ cells. Cells were isolated as described in Fig. 1. Note the decrease of P-ERK in Ter119⁺ cells, which is coincident to the onset of hemoglobinization. B, ERK phosphorylation response of UCP2 KO and WT mice to PH-induced hemolytic anemia during the acute marrow response. Mice were induced to undergo hemolytic anemia as described in Fig. 2. Whole bone marrow samples were collected at D0, D2, and D3 and analyzed by Western blot. For densitometry, P-ERK was normalized to both Porin and total ERK (see "Results") and expressed in relative units (RU). UCP2 KO has significantly reduced levels of P-ERK ($p = 0.0281$, 2-way analysis of variance) at all time points. Error bars represent S.D. C, analysis of P-ERK during *in vitro* erythroid differentiation. TER119⁻ cells were isolated from E13.5 fetal liver as described above and induced to differentiate for 24 h (EPO-dependent phase). Western blot analysis was performed on freshly isolated TER119⁻ cells, and after 24 h in the presence of EPO, they differentiated into TER119⁺ cells. Upon induction of differentiation with EPO, P-ERK was reduced in both WT and UCP2 KO cells as we have seen in bone marrow (A). However, cells from UCP2 KO exhibited an enhanced reduction of P-ERK as compared with WT.

ation either in the presence of pro-oxidants or antioxidants. Paraquat, a pro-oxidant, enhanced cell proliferation and maturation in UCP2 KO cells, exhibiting a rescue effect of UCP2 deficiency. Conversely, TBAP inhibited erythropoiesis, arresting or delaying cells at the R2 stage. These data suggest that UCP2 modulates the cell redox environment and consequently cell expansion.

The function of ROS as a second messenger during erythropoiesis has been reported previously; ROS regulates the MAPK/ERK pathway, activation of which is critical to maintaining the proliferative capability of progenitor cells (38, 61, 62). ROS were

shown to be generated in response to EPO (52, 63), leading to the stimulation of the Ras/MAPK/ERK pathway (39).

We have hypothesized that deficiency of UCP2 directly impacts MAPK/ERK cascade signaling. Both *in vivo* and *in vitro* differentiation experiments showed that UCP2 KO samples have a diminished amount of phosphorylated ERK as compared with WT. This result would explain why UCP2 KO proerythroblast cells divide at a lower rate than WT cells, and it identifies a link between UCP2 and ERK activation in erythropoiesis. UCP2 might modulate ERK phosphorylation and dephosphorylation through ROS signaling and act as a molecular switch. The possibility that UCP2 regulates MAPK/ERK pathway is further supported by the reports, indicating that phosphorylation of ERK-1 and ERK-2 proteins are modulated by O₂⁻ but not H₂O₂ (59, 64), the same ROS species that is modulated by UCP2 (20).

A relationship between UCP2 and the MAPK/ERK pathway has been demonstrated in the elevated inflammatory response which was found in UCP2 KO macrophages after a lipopolysaccharide injection (16, 65). Here we report the UCP2-MAPK/ERK interaction in erythropoiesis, with an effect on cell proliferation during the EPO-dependent phase both *in vivo* and *in vitro*.

Our experiments did not identify an antioxidant role for UCP2 in erythroid heme biosynthesis. In turn, we demonstrate that UCP2 has a role early in erythropoiesis, specifically during the EPO-dependent phase, where it likely controls the amount of ROS available for the activation of MAPK/ERK pathway and, thus, modulates cell proliferation and maturation.

Acknowledgments—We thank Alex Sheftel and Prem Ponka for help with iron incorporation experiments. We thank Solomon Graf and Dani Dagan for critical discussions and for comments on the manuscript. We thank Prem Ponka, Barbara Corkey, Gingbo Pi, and Thorsten Schlaeger for thoughtful and useful advice.

REFERENCES

- Sluse, F. E., Jarmuszkiewicz, W., Navet, R., Douette, P., Mathy, G., and Sluse-Goffart, C. M. (2006) *Biochim. Biophys. Acta* **1757**, 480–485
- Esteves, T. C., and Brand, M. D. (2005) *Biochim. Biophys. Acta* **1709**, 35–44
- Ricquier, D., Miroux, B., Larose, M., Cassard-Doulcier, A. M., and Bouillaud, F. (2000) *Int. J. Obes. Relat. Metab. Disord.* **24**, Suppl. 2, 86–88
- Nicholls, D. G. (2006) *Biochim. Biophys. Acta* **1757**, 459–466
- Krauss, S., Zhang, C. Y., and Lowell, B. B. (2005) *Nat. Rev. Mol. Cell Biol.* **6**, 248–261
- Fleury, C., Neverova, M., Collins, S., Raimbault, S., Champigny, O., Levi-Meyrueis, C., Bouillaud, F., Seldin, M. F., Surwit, R. S., Ricquier, D., and Warden, C. H. (1997) *Nat. Genet.* **15**, 269–272
- Pecqueur, C., Couplan, E., Bouillaud, F., and Ricquier, D. (2001) *J. Mol. Med.* **79**, 48–56
- Pecqueur, C., ves-Guerra, M. C., Gelly, C., Levi-Meyrueis, C., Couplan, E., Collins, S., Ricquier, D., Bouillaud, F., and Miroux, B. (2001) *J. Biol. Chem.* **276**, 8705–8712
- Arsenijevic, D., Onuma, H., Pecqueur, C., Raimbault, S., Manning, B. S., Miroux, B., Couplan, E., ves-Guerra, M. C., Gubern, M., Surwit, R., Bouillaud, F., Richard, D., Collins, S., and Ricquier, D. (2000) *Nat. Genet.* **26**, 435–439
- Negre-Salvayre, A., Hirtz, C., Carrera, G., Cazenave, R., Troly, M., Salvayre, R., Penicaud, L., and Casteilla, L. (1997) *FASEB J.* **11**, 809–815
- Echtay, K. S., Murphy, M. P., Smith, R. A., Talbot, D. A., and Brand, M. D.

- (2002) *J. Biol. Chem.* **277**, 47129–47135
12. Teshima, Y., Akao, M., Jones, S. P., and Marban, E. (2003) *Circ. Res.* **93**, 192–200
 13. Fridell, Y. W., Sanchez-Blanco, A., Silvia, B. A., and Helfand, S. L. (2005) *Cell Metab.* **1**, 145–152
 14. ves-Guerra, M. C., Rousset, S., Pecqueur, C., Mallat, Z., Blanc, J., Tedgui, A., Bouillaud, F., Cassard-Doulcier, A. M., Ricquier, D., and Miroux, B. (2003) *J. Biol. Chem.* **278**, 42307–42312
 15. Li, L. X., Skorpen, F., Egeberg, K., Jorgensen, I. H., and Grill, V. (2001) *Biochem. Biophys. Res. Commun.* **282**, 273–277
 16. Bai, Y., Onuma, H., Bai, X., Medvedev, A. V., Misukonis, M., Weinberg, J. B., Cao, W., Robidoux, J., Floering, L. M., Daniel, K. W., and Collins, S. (2005) *J. Biol. Chem.* **280**, 19062–19069
 17. Nishio, K., Qiao, S., and Yamashita, H. (2005) *J. Mol. Histol.* **36**, 35–44
 18. Brand, M. D., Affourtit, C., Esteves, T. C., Green, K., Lambert, A. J., Miwa, S., Pakay, J. L., and Parker, N. (2004) *Free Radic. Biol. Med.* **37**, 755–767
 19. Conti, B., Sugama, S., Lucero, J., Winsky-Sommerer, R., Wirz, S. A., Maher, P., Andrews, Z., Barr, A. M., Morale, M. C., Paneda, C., Pemberton, J., Gaidarova, S., Behrens, M. M., Beal, F., Sanna, P. P., Horvath, T., and Bartfai, T. (2005) *J. Neurochem.* **93**, 493–501
 20. Mattiasson, G., Shamloo, M., Gido, G., Mathi, K., Tomasevic, G., Yi, S., Warden, C. H., Castilho, R. F., Melcher, T., Gonzalez-Zulueta, M., Nikolich, K., and Wieloch, T. (2003) *Nat. Med.* **9**, 1062–1068
 21. Paradis, E., Clavel, S., Bouillaud, F., Ricquier, D., and Richard, D. (2003) *Trends Mol. Med.* **9**, 522–525
 22. Richard, D., Clavel, S., Huang, Q., Sanchis, D., and Ricquier, D. (2001) *Biochem. Soc. Trans.* **29**, 812–817
 23. Blanc, J., ves-Guerra, M. C., Esposito, B., Rousset, S., Gourdy, P., Ricquier, D., Tedgui, A., Miroux, B., and Mallat, Z. (2003) *Circulation* **107**, 388–390
 24. Polonsky, K. S., and Semenkovich, C. F. (2001) *Cell* **105**, 705–707
 25. Suh, Y. H., Kim, S. Y., Lee, H. Y., Jang, B. C., Bae, J. H., Sohn, J. N., Bae, J. H., Suh, S. I., Park, J. W., Lee, K. U., and Song, D. K. (2004) *J. Endocrinol.* **183**, 133–144
 26. Zhang, C. Y., Baffy, G., Perret, P., Krauss, S., Peroni, O., Grujic, D., Hagen, T., Vidal-Puig, A. J., Boss, O., Kim, Y. B., Zheng, X. X., Wheeler, M. B., Shulman, G. I., Chan, C. B., and Lowell, B. B. (2001) *Cell* **105**, 745–755
 27. Shirihai, O. S., Gregory, T., Yu, C., Orkin, S. H., and Weiss, M. J. (2000) *EMBO J.* **19**, 2492–2502
 28. Ryter, S. W., and Tyrrell, R. M. (2000) *Free Radic. Biol. Med.* **28**, 289–309
 29. Greenberg, P. L., Young, N. S., and Gattermann, N. (2002) *Hematology Am. Soc. Hematol. Educ. Program* **2002**, 136–161
 30. Fontenay, M., Cathelin, S., Amiot, M., Gyan, E., and Solary, E. (2006) *Oncogene* **25**, 4757–4767
 31. Craven, S. E., French, D., Ye, W., de, S. F., and Rosenthal, A. (2005) *Blood* **105**, 3528–3534
 32. Friedman, J. S., Rebel, V. I., Derby, R., Bell, K., Huang, T. T., Kuypers, F. A., Epstein, C. J., and Burakoff, S. J. (2001) *J. Exp. Med.* **193**, 925–934
 33. Friedman, J. S., Lopez, M. F., Fleming, M. D., Rivera, A., Martin, F. M., Welsh, M. L., Boyd, A., Doctrow, S. R., and Burakoff, S. J. (2004) *Blood* **104**, 2565–2573
 34. Martin, F. M., Bydlon, G., and Friedman, J. S. (2006) *Antioxid. Redox Signal.* **8**, 1217–1225
 35. Lee, T. H., Kim, S. U., Yu, S. L., Kim, S. H., Park, D. S., Moon, H. B., Dho, S. H., Kwon, K. S., Kwon, H. J., Han, Y. H., Jeong, S., Kang, S. W., Shin, H. S., Lee, K. K., Rhee, S. G., and Yu, D. Y. (2003) *Blood* **101**, 5033–5038
 36. Lebovitz, R. M., Zhang, H., Vogel, H., Cartwright, J., Jr., Dionne, L., Lu, N., Huang, S., and Matzuk, M. M. (1996) *Proc. Natl. Acad. Sci. U. S. A.* **93**, 9782–9787
 37. Li, Y., Huang, T. T., Carlson, E. J., Melov, S., Ursell, P. C., Olson, J. L., Noble, L. J., Yoshimura, M. P., Berger, C., Chan, P. H., Wallace, D. C., and Epstein, C. J. (1995) *Nat. Genet.* **11**, 376–381
 38. Zhang, J., and Lodish, H. F. (2004) *Blood* **104**, 1679–1687
 39. Iiyama, M., Kakihana, K., Kurosu, T., and Miura, O. (2006) *Cell. Signal.* **18**, 174–182
 40. Bugariski, D., Krstic, A., Mojsilovic, S., Vlaski, M., Petakov, M., Jovcic, G., Stojanovic, N., and Milenkovic, P. (2007) *Exp. Biol. Med. (Maywood)* **232**, 156–163
 41. Zhang, J., Socolovsky, M., Gross, A. W., and Lodish, H. F. (2003) *Blood* **102**, 3938–3946
 42. Beauchemin, H., Blouin, M. J., and Trudel, M. (2004) *J. Biol. Chem.* **279**, 19471–19480
 43. Rossi, R., Giustarini, D., Milzani, A., and le-Donne, I. (2006) *Blood Cells Mol. Dis.* **37**, 180–187
 44. Khanna, R., Chang, S. H., Andrabi, S., Azam, M., Kim, A., Rivera, A., Brugnara, C., Low, P. S., Liu, S. C., and Chishti, A. H. (2002) *Proc. Natl. Acad. Sci. U. S. A.* **99**, 6637–6642
 45. Socolovsky, M., Nam, H., Fleming, M. D., Haase, V. H., Brugnara, C., and Lodish, H. F. (2001) *Blood* **98**, 3261–3273
 46. Zhang, A. S., Sheftel, A. D., and Ponka, P. (2005) *Blood* **105**, 368–375
 47. Martinez-Medellin, J., and Schulman, H. M. (1972) *Biochim. Biophys. Acta* **264**, 272–274
 48. Rooke, H. M., and Orkin, S. H. (2006) *Blood* **107**, 3527–3530
 49. Kefaloyianni, E., Gaitanaki, C., and Beis, I. (2006) *Cell. Signal.* **18**, 2238–2251
 50. Gregory, T., Yu, C., Ma, A., Orkin, S. H., Blobel, G. A., and Weiss, M. J. (1999) *Blood* **94**, 87–96
 51. Chen, J. J. (2007) *Blood* **109**, 2693–2699
 52. Cakir, Y., and Ballinger, S. W. (2005) *Antioxid. Redox Signal.* **7**, 726–740
 53. Flachs, P., Sponarova, J., Kopecky, P., Horvath, O., Sediva, A., Nibelink, M., Casteilla, L., Medrikova, D., Neckar, J., Kolar, F., and Kopecky, J. (2007) *FEBS Lett.* **581**, 1093–1097
 54. Muta, K., Krantz, S. B., Bondurant, M. C., and Dai, C. H. (1995) *Blood* **86**, 572–580
 55. Koury, M. J., and Bondurant, M. C. (1988) *J. Cell Physiol.* **137**, 65–74
 56. Wu, H., Klingmuller, U., Besmer, P., and Lodish, H. F. (1995) *Nature* **377**, 242–246
 57. de, B. F., Arsenijevic, D., Vallet, P., Hjelle, O. P., Ottersen, O. P., Bouras, C., Raffin, Y., Abou, K., Langhans, W., Collins, S., Plamondon, J., ves-Guerra, M. C., Haguenaer, A., Garcia, I., Richard, D., Ricquier, D., and Giannakopoulos, P. (2004) *J. Neurochem.* **89**, 1283–1292
 58. Sears, R. C., and Nevins, J. R. (2002) *J. Biol. Chem.* **277**, 11617–11620
 59. Genestra, M. (2007) *Cell. Signal.* **19**, 1807–1819
 60. Pecqueur, C., Bui, T., Gelly, C., Hauchard, J., Barbot, C., Bouillaud, F., Ricquier, D., Miroux, B., and Thompson, C. B. (2008) *FASEB J.* **22**, 9–18
 61. Rubiolo, C., Piazzolla, D., Meissl, K., Beug, H., Huber, J. C., Kolbus, A., and Baccarini, M. (2006) *Blood* **108**, 152–159
 62. Thakur, V., Pritchard, M. T., McMullen, M. R., Wang, Q., and Nagy, L. E. (2006) *J. Leukocyte Biol.* **79**, 1348–1356
 63. Sattler, M., Winkler, T., Verma, S., Byrne, C. H., Shrikhande, G., Salgia, R., and Griffin, J. D. (1999) *Blood* **93**, 2928–2935
 64. Baas, A. S., and Berk, B. C. (1995) *Circ. Res.* **77**, 29–36
 65. Emre, Y., Hurtaud, C., Nubel, T., Criscuolo, F., Ricquier, D., and Cassard-Doulcier, A. M. (2007) *Biochem. J.* **402**, 271–278